Multi-objective Design Optimization for Current Sensor Rogowski Coil

Xia Du
Department of Electrical Engineering
University of Arkansas
Fayetteville, USA
xiadu@uark.edu

Andrea Stratta
Department of Electrical and Electronic Engineering
University of Nottingham
Nottingham, UK
astratta@uark.edu

David Arturo Porras Fernandez
Department of Electrical Engineering
University of Arkansas
Fayetteville, USA
daporras@uark.edu

Yuqi Wei
Department of Electrical Engineering
University of Arkansas
Fayetteville, USA
yuqiwei@uark.edu

Yuheng Wu
Department of Electrical Engineering
University of Arkansas
Fayetteville, USA
yuhengwu@uark.edu

Zahra Saadatizadeh
Department of Electrical Engineering
University of Arkansas
Fayetteville, USA
zahras@uark.edu

Chris Farnell
Department of Electrical Engineering
University of Arkansas
Fayetteville, USA
cfarnell@uark.edu

H. Alan Mantooth
Department of Electrical Engineering
University of Arkansas
Fayetteville, USA
mantooth@uark.edu

***Abstract*— This paper discusses the possibility of using a multi-objective optimization workflow to design Rogowski coil current sensor and optimize its performance. Seven geometrical parameters can be used as design variables to maximize objective functions such as sensor bandwidth and sensitivity. Based on the electrical lumped parameter model of the Rogowski coil, the sensor geometry is optimized combining a genetic algorithm (GA) in Matlab and a finite element (FE) electromagnetic model in Q3D Ansys. To validate the proposed design approach, a compact current sensor with very high bandwidth (up to 300 MHz) is designed, prototyped, tested, and compared with a suboptimal design (up to 100 MHz). Experimental results prove the validity and optimality of the sensor model used for the design.**

Keywords*— *Rogowski coil, current measurement, magnetic field sensor, wide bandwidth, current sensor, finite element method

I. Introduction

With the emerging of wideband gap (WBG) devices, power electronic converters can achieve unprecedented levels of power density and switching frequency. Playing a critical role for the evaluation of switching characteristics, current monitoring for power system optimization, current control for closed loop circuit and overcurrent protection, current sensors are expected to reach the MHz range bandwidth to capture the current waveform faithfully for the power converters with megahertz switching frequency [1]. Furthermore, due to the higher power density, more compact structures and packaging technique improvements, power modules has been widely used in the power converters [2]-[9]. With the limited space and complicated electromagnetic environment within the modules, current sensors are required to have smaller size, competitive structures and strong noise immunity for neater integration without compromising sensing accuracy and reliability [10]-[13]. In addition, the switching transient oscillations, cross talk and overshoot are determined by the power loop parasitic capacitance and inductance, therefore it is vital for the current sensor to be nonintrusive with its stray inductance as small as possible [14],[15]. Besides all the above mentioned, galvanic isolation, wide measurement range, highly robustness in harsh environments and low cost are also need to be taken into account depending on the applications.

There are several commonly used high-bandwidth current sensor [1],[16]. Current shunt resistors are popular because of its low cost and easy integration, and suitable for high current and high bandwidth up to GHz, but they introduce high parasitic inductance to the power loop and result in power loss in the power circuit [17]. They also don't have galvanic isolation. Current transformers can ensure the galvanic isolation and bandwidth can achieve up to 250 MHz, but they suffer from flux saturation and size limitations for compact WBG applications due to the magnetic core characteristics [18]. Rogowski coils are currently drawing more attention because of its potentially broad bandwidth, small volume, high accuracy, and ease of integration [19]-[23]. From traditional helical to common print-circuit-board (PCB) implementations, most of research focus on the winding shape and integrator design, but little on the optimization of Rogowski coil, since most of the designs are only based on an equivalent circuit of the parasitic parameters that are intrinsic to it, which makes it hard to represent and predict all its characteristics in a comprehensively way. Thus, it involves a great amount of non-optimized experimental trial to appropriately select the geometry that will achieve the desired bandwidth and sensitivity. Besides, all the structures of Rogowski coil are in the toroidal or square shape, which is not convenient to integrate into the modules and power circuit [23],[24].

This paper continues to use a novel structure for current sensor in [25]. It is nonintrusive and easy to be integrated into a power stage or modules. Numerical integration or analog integration can both be applied. Based on the structure, Finite Element Method (FEM) simulations are executed in Ansys Q3D combining with a genetic algorithm in Matlab to investigate the effects that the geometrical parameters have on the Rogowski coil key performances: bandwidth and sensitivity. This method allows the simulation of complex coil and primary current conductor geometries, including parasitic inductance and capacitance. Therefore it is possible to simulate the complete system with reasonable computational cost (less than 2 minutes for each simulation).

In the following, first, the novel structure and modeling of the current sensor are briefly introduced, and boundary conditions for simulation are demonstrated. Then an automated design workflow is proposed to optimize the sensor geometry, which include: the sensor electrical lumped parameter model, the finite element electromagnetic model and the genetic algorithm optimization. All the workflow is implemented in the Matlab environment. Finally, to check the validity of the proposed method, experimental validations of the optimization group compared with control group based on double pulse test are presented.

II. Modeling and Design Specifications

A. Modeling of the Proposed Rogowski Coil

Fig. 1 (a) shows the sketch of the being optimized Rogowski coil structure [25]. The primary current I_{pri} is carried by the conductor, a Ω-shaped brass tube with an extended part, which can be easily integrated within the power circuit or modules. The coil inside the tube, wound on a 3D printed ABS plastic supporter, senses the varying magnetic field generated by the primary changing current, thus resulting in a voltage, notated as U_{emf}, in the windings. According to the Ampere's law (1) and Faraday's law (2):

$$Ni(t) = \frac{1}{u_0} \oint B(t)\, dl \tag{1}$$

$$U(t) = N\frac{d\emptyset}{dt} = N \cdot \int \dot{B}(t) dA = \frac{N^2 \cdot A}{l} u_0 \frac{di}{dt} \tag{2}$$

where N is the number of turns, l is the distance along the coaxial coil, and A is the cross-section for the windings. Based on (2), the induced voltage U_{emf} is proportional to the changing rate of the primary current:

$$U_{emf} = M\frac{di}{dt}, \qquad M = \frac{N^2 \cdot A}{l} u_0 \tag{3}$$

where M is defined as the mutual inductance between the primary current conductor and the secondary Rogowski coil. Therefore, the primary current can be retrieved by integrating the induced voltage U_{emf}. M serves as an indicator for the sensitivity of the Rogowski coil design, which implies the amplitude of the measurement signal displayed on an oscilloscope.

A simplified, lumped parameter model of the proposed Rogowski coil is shown in Fig. 1 (b). It consists of electromotive force U_{emf}, which is induced by the changing primary current, self-inductance of coil L_{coil}, series resistance R_s, parasitic capacitance C_{coil} and terminal resister R_T. After the simulation and bandwidth investigation, it is noticed that parasitic resistance R_s can be neglected for its little effect for the bandwidth design. Therefore, the transfer function of this model can be simplified as shown in (4):

$$G_{Rog}(S) = \frac{1}{L_{coil} \cdot C_{coil} \cdot S^2 + \frac{L_{coil}}{R_T} \cdot S + 1} \tag{4}$$

GRID Connected Advanced Power Electronics Systems.

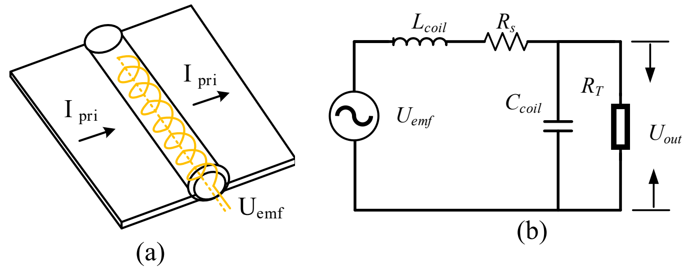

Fig.1. (a) Sketch of a basic inductive current sensor; (b) Modeling of the proposed Rogowski coil.

TABLE I. Boundary Conditions of Design Variabilities

Variations	Size Limitation	
	Minimum(cm)	***Maximum(cm)***
① Length of coil M_L	/	10
② Diameter of air-core supporter M_D	/	1
③ Number of turns (N)	2	20
④ Wire radius (R_{wire})	0.005	0.025
⑤ Distance between coil and tube (*Diso*)	0.01	0.1
⑥ Tube thickness	0.1	0.3
⑦ Pitch	2.1*④	①/③
⑧ Helix radius (R_{coil})	1.8*④	①/2-⑤-⑥
⑨ Aperture	0.005	⑧

The second order system is commonly described in the Laplace domain as follows:

$$G(S) = \frac{k}{\frac{1}{{w_0}^2} \cdot S^2 + \frac{2\zeta}{w_0} \cdot S + 1} \tag{5}$$

where k is the gain of the system, w_0 is the angular frequency and ζ is the damping ratio. The terminal resistor is designed to avoid the overshoots near its resonant frequency, thus R_T is determined when the damping ratio ζ is 1 for a critically damped system. In the design, the parasitic inductance L_{coil}, capacitance C_{coil} can be extracted from Ansys Q3D extractor, then R_T can be calculated according to the transfer function (5) with ζ=1. The bandwidth is defined at the 3 dB point in its transfer function. This paper mainly focuses on the coil geometry design and off-line digital integration is used as an auxiliary.

B. Design Specifications of Simulation

To define the current sensor geometry, there are 7 design parameters: number of turns(N); Pitch, which is the distance between two turns; helix radius (R_{coil}), which is the size of the air-core supporter; wire radius (R_{wire}), which is the thickness of the coil's conductor; isolation distance between coil and tube (D_{iso}); tube wall thickness; Aperture, which is the size of the slot on the copper tube. Consider the size constraints for applications, the maximum length of the Rogowski coil M_L is defined as 10 cm and the maximum diameter of the air-core supporter M_D is set to 1 cm. Based on the size limitation and

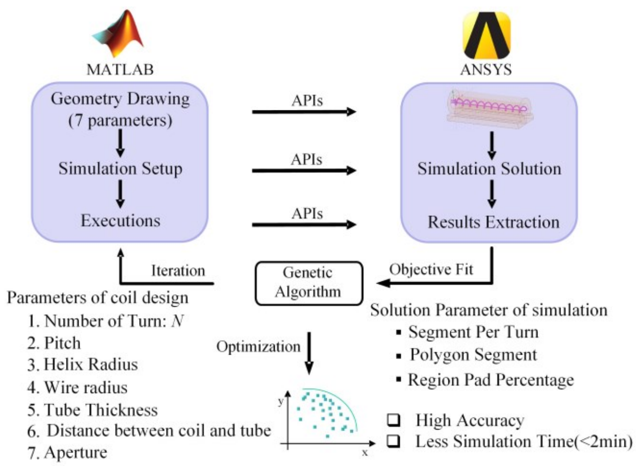

Fig.2. Simulation environment diagram.

physical association in reality, the boundary conditions of all the design variabilities are shown in TABLE I.

III. Optimal Automated Design

To obtain good current sensor performance, the two of the most important attributes are bandwidth and sensitivity. Bandwidth is obtained according to the transfer function as mentioned in section II. According to Faraday's law, to retrieve the primary current I_{pri}:

$$I_{pri} = \frac{1}{M}\int U_{out}\,dt \qquad (6)$$

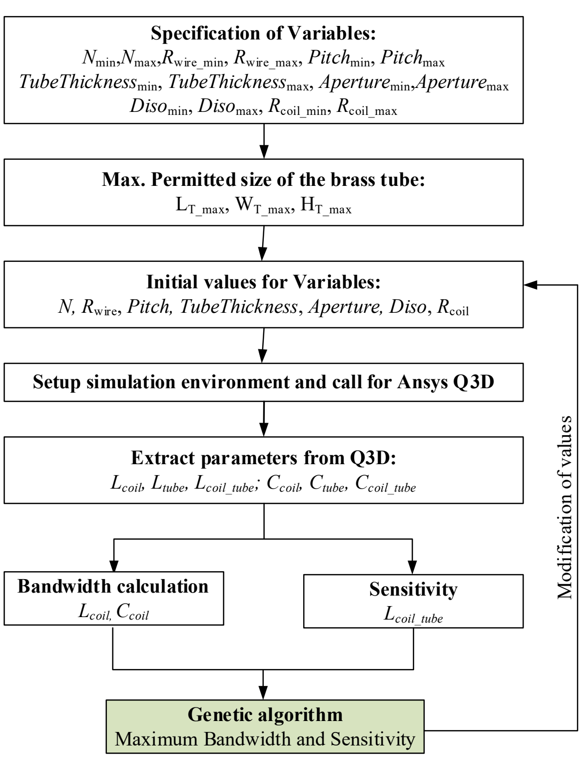

Fig.3. Flowchart for the optimization algorithm.

In real applications, the higher bandwidth, the better the current waveform can be reconstructed; the higher sensitivity M, the easier to measure the signals U_{out}, which is also easier for the integrator design, since the signal-to-noise ratio (SNR) will be larger. However, there is a compromise between these two attributes.

By considering the tradeoff between the bandwidth and the sensitivity, an optimization algorithm based on a multi-objective stochastic population-based optimization algorithm (NSGA-II embedded in MATLAB environment) combining with finite element method in ANSYS is developed to find the optimal combinations of design variables shown as the diagram in Fig.2. In the genetic algorithm, a population of randomly generated combination of 7 design variables to the optimization objectives is evolved toward better solutions by an iterative process. With the population in each iteration called a generation. A new generation is formed according to the fitness of individuals stochastically selected from the current population. Commonly, the algorithm terminates when either a maximum number of generations has been produced, or a satisfactory fitness level has been reached for the population.

To minimize the computational cost of the simulation, three environment variations: segment per turn for the Ω-shaped brass tube, polygon segment for the windings and region pad percentage for the vacuum region of the simulation boundary, are investigated to keep the simulation time less than 2 minutes per loop. With the simulation, the polygon segment and region pad percentage don't affect the simulation time significantly. Finally polygon segment and region pad percentage are set up as 20 with 0.53% error for Bandwidth and 1.42% error for mutual inductance, polygon segment is set up as 6 with 0.2% error for Bandwidth and 0.8% error for mutual inductance to minimize the simulation time to 1.23 minutes per iteration.

As shown in the flowchart in Fig. 3, based on the boundary conditions and initial values of the design variables, Matlab will call for Ansys Q3D to draw the geometry of the Rogowski coil

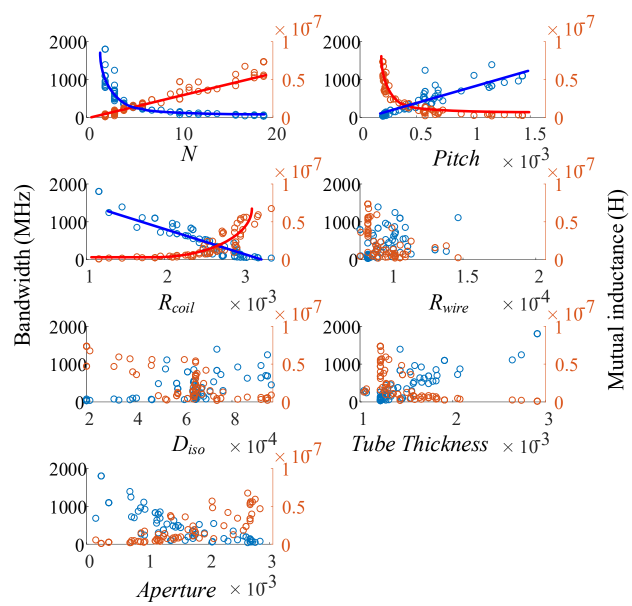

Fig.4. Geometrical parameters' effects on objectives.

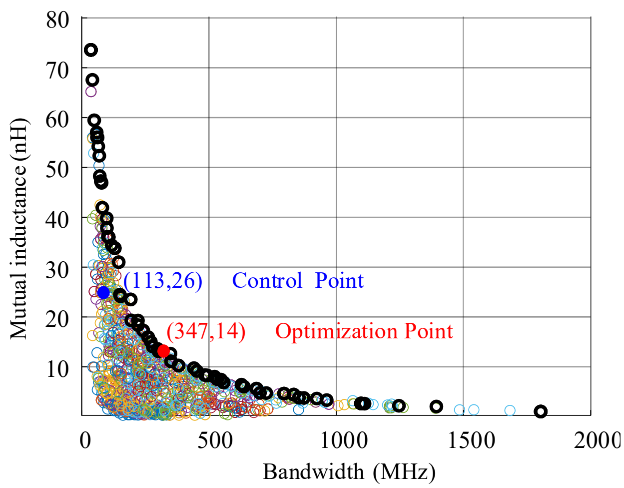

Fig.5. Optimized simulation results.

and do the simulation to extract parasitic parameters to calculate the bandwidth and mutual inductance through Application Programming Interfaces (APIs). Once the performance indexes are calculated, a fitness function shown as in (7) is applied to evaluate the solution.

$$Min\left(\frac{1}{Bandwidth},\frac{1}{M}\right) \tag{7}$$

The iterative optimization terminates when it reaches the maximum generation. In this algorithm, the generation and population are defined as 50 and 100, respectively.

To have a better understanding of how all the seven design variables affect the design objectives, Fig.4 summaries the simulation results. The effect of number of turns N on the bandwidth and mutual inductance can be seen in the first graph: with the increasing of N, bandwidth is decreasing and mutual inductance is increasing. The most significant trends are highlighted with a solid red line for mutual inductance and a solid blue line for bandwidth. Similarly, *Pitch* and Helix radius R_{coil} also have a dominant effect on the performance indexes. However, for Wire radius R_{wire}, Distance between coil and tube D_{iso}, *Tube thickness* and *Aperture*, there is a broad data dispersion, which means that these design variables don't have a significant effect on the design objectives. Principally, it is worth noting that there is always a tread off between the bandwidth and mutual inductance.

To find the optimization points for the two design objectives, all the simulated scenarios results (colored marked dots) are shown in Fig.5. Each dot marker corresponds to a different combination of the seven geometry parameters. It is obvious that there is compromise between the bandwidth and the sensitivity. The optimal design points (black marker dots) form the Pareto-front, which are considered optimal solutions. On this curve in Fig. 5, it is possible to maximize bandwidth at the expense of sensitivity or maximize sensitivity at the expense of bandwidth, but they cannot be both improved at once. The selected optimization point is the one that offers good compromise between bandwidth and sensitivity (red marker dot).

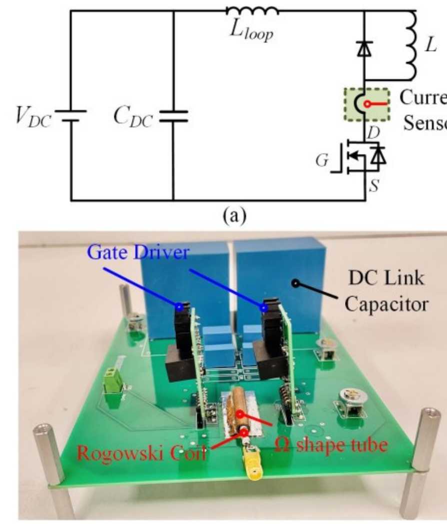

(b)

Fig.6. Experimental Setup

IV. Experimental Validation

A double pulse test was carried out to validate the proposed optimization design of the Rogowski coil. The double pulse test schematic and test bench is shown as Fig. 6 (a) and (b). The Ω copper tube is sitting between the upper and lower MOSFET switch 1.2kV/63A SiC MOSFET (C2M0025120D) from CREE, where the switching current have to go through. In experiment, the upper switch works as a freewheeling diode. When the drain current goes through the tube, the self-design Rogowski coil will pick up the magnetic file and display the terminal voltage in the oscilloscope directly through the SMA connector. This data will be collected to do the off-line digital integration and is compared to commercial Rogowski coil with 30 MHz bandwidth from PEM for verification.

To validate the theoretical analysis, two combinations of design variables consisting of the optimization group and control group are tested on a double pulse test experiment with

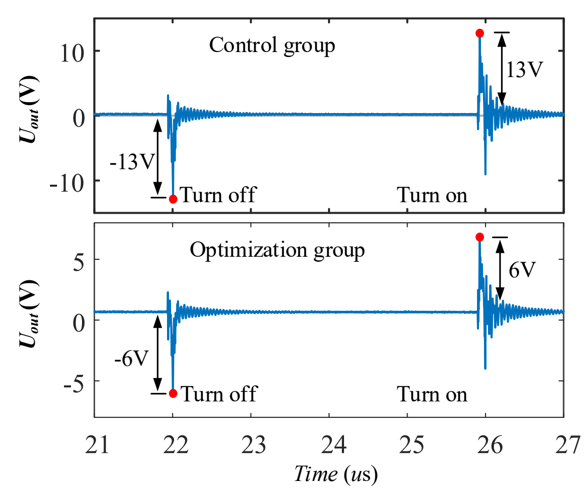

Fig.7. Terminal voltage of Rogowski coil

TABLE II. PARAMETERS OF COMPARISON GROUPS

Variations	Comparison groups		3D Support of Rogowski Coil	
	Optimization group	Control group	Optimization group	Control group
① Number of turns(N)	4	9	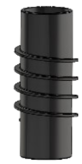	
② Pitch	0.3 mm	0.5 mm		
③ Helix radius (R_{coil})	3 mm	2.5 mm		
Mutual inductance(M)	14 nH	26 nH		
Bandwidth	347 MHz	113 MHz		

a DC bus voltage of 200V and a load current of 40 A. The control group was a suboptimal design before the optimization process and is shown to check the validity of the optimization group. When the mutual inductance is too low and bandwidth is high, difficulty of integrator design will increase rapidly because of the weak coupling between the primary side and secondary side, therefore, there is no control group in high bandwidth and low mutual inductance areas. Since the Ansys simulation shows mainly number of turns, Pitch and coil radius have significant effect on the two objectives, the parameters of these two groups are shown in TABLE II.

To restore the primary current, the voltage induced in the terminal of the coil is processed as follows: 1) Subtracting of a DC component by Fast Fourier Transform (FFT) analysis of the original signal; 2) Integrating the electromagnetic voltage; 3) Compensating of the propagation delay; 4) Scaling of the amplitude of the integrated signal to an externally measured current amplitude. The experimental results are shown in Fig.7 and Fig. 8. The maximum terminal voltage U_{out} is around 6 V for optimization group, 13 V for control group, which matches with the mutual inductance ratio 14:26 obtained from Ansys simulation. The gain ratio of the digital integration to scale the measurement up is 120:250, which further proved the feasibility and effectiveness of the optimization method. In Fig. 8, the fully reconstructed details of the current compared with the commercial Rogowski coil verify that the bandwidth is high enough for switching current.

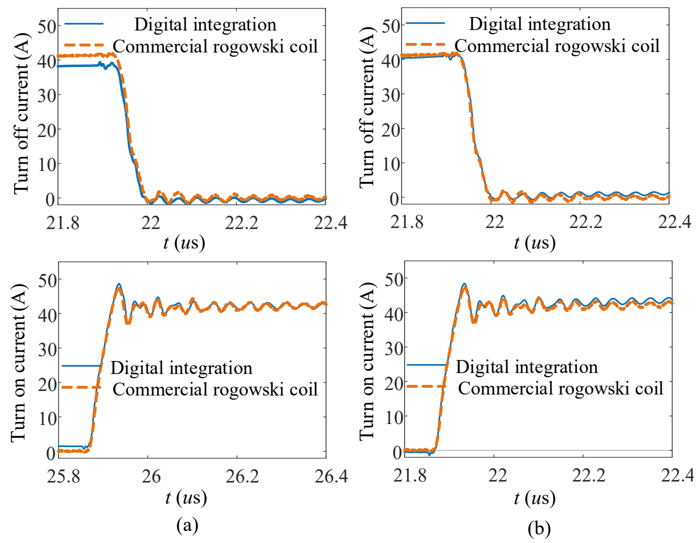

Fig. 8. Experimental results (a) Control group; (b) Optimization group.

V. CONCLUSIONS

In this paper, a multi-objective design optimization based on the Rogowski coil geometry is presented. With the genetic algorithm in Matlab combining the finite element electromagnetic models in Q3D Ansys, the good compromise between bandwidth and sensitivity can be optimized. Finally, the experimental results for an optimal design compared with a non-optimal design are validated under a double pulse test with DC link voltage 200 V and drain current 40 A. All the oscillations of the current during switching transient can be reconstructed in details compared with the commercial Rogowski coil.

ACKNOWLEDGMENT

This material is based upon work supported by the National Science Foundation under Grant No. 1939144, GRID Connected Advanced Power Electronics Systems (GRAPES), Project GR-21-06. Any opinions, findings, and conclusions or recommendations expressed in this material are those of the author(s) and do not necessarily reflect the views of the National Science Foundation.

REFERENCES

[1] Z. Xin, H. Li, Q. Liu and P. C. Loh, "A Review of Megahertz Current Sensors for Megahertz Power Converters," *IEEE Trans. Power Electron.*, vol. 37, no. 6, pp. 6720-6738, June 2022.

[2] Z. Huang et al., "A Novel Low Inductive 3D SiC Power Module Based on Hybrid Packaging and Integration Method," *IEEE Energy Convers. Congr. Expo.*, pp. 3995–4002, 2017.

[3] F. Hou et al., "Review of Packaging Schemes for Power Module," *IEEE Trans. Emerg. Sel. Topics Power Electron.*, vol. 8, no. 1, pp. 223–238, Mar. 2020.

[4] L. Du and J. He, "A Simple Autonomous Phase-Shifting PWM Approach for Series-Connected Multi-Converter Harmonic Mitigation," *IEEE Trans. Power Electron*., vol. 34, no. 12, pp. 11516-11520, Dec. 2019.

[5] J. He, L. Du, B. Liang, Y. Li and C. Wang, "A Coupled Virtual Impedance for Parallel AC/DC Converter Based Power Electronics System," *IEEE Trans. on Smart Grid*, vol. 10, no. 3, pp. 3387-3400, May 2019.

[6] J. He, L. Du, S. Yuan, C. Zhang and C. Wang, "Supply Voltage and Grid Current Harmonics Compensation Using Multi-Port Interfacing Converter Integrated Into Two-AC-Bus Grid," *IEEE Trans. on Smart Grid*, vol. 10, no. 3, pp. 3057-3070, May 2019.

[7] Y. Chen, L. Du and J. He, "Online Diagnosis and Ride-Through Operation for Cascaded H-Bridge Converter Based STATCOM With a Single Open-Circuit IGBT," *IEEE Trans. Ind. Electron.*, vol. 69, no. 8, pp. 7549-7559, Aug. 2022.

[8] F. Guo, T. Yang, C. Li, S. Bozhko and P. Wheeler, "Active Modulation Strategy for Capacitor Voltage Balancing of Three-Level Neutral-Point-Clamped Converters in High-Speed Drives," *IEEE Trans. Ind. Electron*., vol. 69, no. 3, pp. 2276-2287, Mar. 2022.

[9] F. Guo, T. Yang, A. M. Diab, S. S. Yeoh, S. Bozhko and P. Wheeler, "An Enhanced Virtual Space Vector Modulation Scheme of Three-Level NPC Converters for More-Electric-Aircraft Applications," *IEEE Trans. Ind. Appl.*, vol. 57, no. 5, pp. 5239-5251, Sept.-Oct. 2021.

[10] K. Hasegawa, S. Sho, M. Tsukuda, I. Omura, M. Ichiki, and T. Kato, "Output-current Measurement of a PWM Inverter With a Tiny PCB Rogowski Sensor Integrated Into an IGBT Module," *IEEE Energy Convers. Congr. Expo.,* pp. 5707–5711, Sep. 2019.

[11] M. Sheng, M. H. Alvi, and R. D. Lorenz, "20 MHz Integrated Current Sensing for WBG Systems With EMI Suppression," *IEEE Energy Convers. Congr. Expo.*, pp. 375–382, Sep. 2018.

[12] H. Chen, M. Hossain, D. G. Castillo, X. Li, A. Wallace, Y. Chen, H. A. Mantooth, "Design and Optimization of SiC MOSFET Wire Bondless Power Modules," *2020 IEEE 9th International Power Electronics and Motion Control Conference* (IPEMC2020-ECCE Asia), pp. 725-728, 2020.

[13] H. Chen, T. Wei, Y. Chen, X. Li, N. Li, Q. Zhu, S. Hazra, Y. Zhao, M. P. Gupta, M. Asheghi, Y. Lu, K. Goodson, H. A. Mantooth, "Feasibility Design of Tight Integration of Low Inductance SiC Power Module with Microchannel Cooler," *IEEE Appl. Power Electron. Conf. Expo.*, pp. 962-965, Mar. 2022.

[14] N. Tröster, J. Wölfle, J. Ruthardt, and J. Roth-Stielow, "High Bandwidth Current Sensor With a Low Insertion Inductance based on the HOKA Principle," *Eur. Conf. Power Electron*. pp. 1–9, Appl., Sep. 2017.

[15] L. Shillaber, L. Ran, Y. Shen, and T. Long, "Gigahertz Current Measurement for Wide Band-gap Devices," *IEEE Energy Convers. Congr. Expo.*, pp. 2357–2363, Oct. 2020.

[16] F. Costa, P. Poulichet, F. Mazaleyrat, and E. Laboure, "The Current Sensors in Power Electronics, a Review," *Eur. Power Electron. Drives J.*, vol. 11, pp. 7–18, Sep. 2015.

[17] W. Zhang, Z. Zhang, F. Wang, E. V. Brush, and N. Forcier, "Highbandwidth Low-inductance Current Shunt for Wide-bandgap Devices Dynamic Characterization," *IEEE Trans. Power Electron*., vol. 36, no. 4, pp. 4522–4531, Apr. 2021.

[18] Pearson Electronics, "Pearson Current Monitor," 2021. [Online]. Available: https://www.pearsonelectronics.com/pdf/7713-03.pdf

[19] Yan Wang, Xiaoshe Zhai, Zhengxiang Song and Yingsan Geng, "A New Method to Detect The Short Circuit Current in DC Supply System based on the Flexible Rogowski Coil," *2011 1st International Conference on Electric Power Equipment - Switching Technology*, pp. 237-240, 2011.

[20] R. Han, J. Wu, W. Ding, Y. Jing, H. Zhou, Q. Liu, and Ai. Qiu, "Hybrid PCB Rogowski Coil for Measurement of Nanosecond-Risetime Pulsed Current," *IEEE Trans. Plasma Science*, vol. 43, no. 10, pp. 3555-3561, Oct. 2015.

[21] M. H. Samimi, A. Mahari, M. A. Farahnakian and H. Mohseni, "The Rogowski Coil Principles and Applications: A Review," *IEEE Sens. J.,* vol. 15, no. 2, pp. 651-658, Feb. 2015.

[22] Y. Shi, Z. Xin, P. C. Loh and F. Blaabjerg, "A Review of Traditional Helical to Recent Miniaturized Printed Circuit Board Rogowski Coils for Power-Electronic Applications," *IEEE Trans. Power Electronics*., vol. 35, no. 11, pp. 12207-12222, Nov. 2020.

[23] W. Zhang, S. B. Sohid, F. Wang, H. Cui and B. Holzinger, "High-Bandwidth Combinational Rogowski Coil for SiC MOSFET Power Module," *IEEE Trans. Power Electron.,* vol. 37, no. 4, pp. 4397-4405, Apr. 2022.

[24] T. Guillod, D. Gerber, J. Biela and A. Muesing, "Design of a PCB Rogowski Coil based on the PEEC Method," *2012 7th International Conference on Integrated Power Electronics Systems* (CIPS), pp. 1-6, 2012.

[25] Stippich Alexander (2021). Exploiting the Full Potential of Silicon Carbide Devices via Optimized Highly Integrated Power Modules [Doctoral dissertation, RWTH Aachen University].